ELSEVIER

Biophysical Chemistry 53 (1995) 227–239

Biophysical Chemistry

# Influence of ligands on the fluorescence polarisation anisotropy of ethidium bound to DNA

Maddalena Collini, Giuseppe Chirico, Giancarlo Baldini *

*Università degli Studi di Milano, Dipartimento di Fisica, Via Celoria 16, 20133-I, Italy*

Received 5 May 1994; accepted in revised form 5 July 1994

**Abstract**

The decay of the fluorescence polarisation anisotropy (FPA) of the ethidium–DNA complex has been measured by multifrequency phase fluorometry, in order to study the perturbations induced by the presence of different ligands on the torsional dynamics of DNA, a moderately flexible polymer that undergoes bending (flexure of the helix axis) and torsional (twisting of base pairs) motions. Two probes have been used together with ethidium: an intercalator, chloroquine, and a minor groove binding dye: hoechst 33258. Chloroquine is found to substantially modify the DNA torsional dynamics both in linear and in circularly closed DNAs only at high binding ratios, in agreement with previous reports [Wu et al. Biochem. 27 (1988) 8128]. The effective elastic constant becomes approximately three times larger when the dye/base pairs binding ratio is higher than 0.14. The minor groove ligand hoechst 33258, on the other hand, greatly increases the effective elastic constant to the point that at dye/base pairs ratios larger than 0.5, the effective elastic constant becomes stiffer by several orders of magnitude, suggesting a progressive hindering of internal motions. The results reported here show that DNA torsions are more effectively influenced by groove-binding molecules than by intercalators and it is expected that the large perturbation of the former ligand may be useful when describing the change in the dynamical properties induced by DNA binding proteins. FPA in the frequency domain, the technique adopted throughout this work, has proved to be very sensitive to changes of the elastic constant that describes DNA torsional dynamics. Several computer simulations performed in order to predict the FPA time decay of intercalated ethidium have led to good agreement with the observed results.

*Keywords*: Fluorescence polarisation anisotropy; Frequency modulation; DNA torsional dynamics; Hoechst 33258; Ethidium

## 1. Introduction

The understanding of the dynamical properties of DNA has made significant progress in recent years due mainly to the development of experimental and theoretical methods. In particular, concerning the experimental methods, a few techniques such as light scattering [1,2] electric [3,4] and magnetic birefringence [5] and NMR relaxation [6] have become available. The dynamical processes that can be explored with these techniques concern the traslational and rotational motions together with some other slow internal motions whose associated characteristic times range from 1 μs to 1 ms. Faster motions of DNA can also be studied by means of other techniques that can follow the time response of appropriate probes. Concerning this point interesting results have been obtained by studying the fluorescence anisotropy decay of well known DNA ligands (ethidium, chloroquine, etc.). Investigations of sample systems, constituted by dye

* Corresponding author.


*SSDI* 0301-4622(94)00099-9

intercalated DNA, can be employed also for the study of DNA or RNA dynamics in the presence of proteins. The use of fluorescent probes selects the range that can be studied, from 0.1 to 100 ns, a range that corresponds to the characteristic times of the DNA torsional motions. Attention has been reported also for slower motions by means of the triplet anisotropy decay of methylene blue, a probe which permits studies of DNA motions 1000 times slower than those explored by fluorescence [7–9]. From the above techniques, DNA elastic parameters, such as the torsional and bending rigidity, can be derived.

The early theories describing the internal motions of a macromolecule, due to Rouse and Zimm [10,11], took into account only the long coil deformation motions. Recently more general theories have become available in order to describe the whole DNA dynamical spectrum, in particular the (faster) torsional motions and the (slower) bending motions [12–14]. If DNA bending and torsional motions can be considered uncoupled, then an analytical expression can be derived [12] for the torsional angles correlation function. Since torsional and bending motions usually involve different characteristic relaxation times, it is then possible to investigate separately each contribution. In this work we have dealt with a probe, ethidium bromide (EB), whose lifetime is about 20 ns and with DNA whose length is 2700 base pairs or more, a combination that is suitable for investigating the torsional dynamics of DNA. The torsional properties of DNA can then be measured by monitoring the fluorescence anisotropy decay of the intercalated dye.

Frequency modulated fluorescence polarisation anisotropy (FPA) was recently applied to the study of DNA–dye complexes and found useful in determining the torsional constant of a linear standard calf thymus DNA intercalated with ethidium bromide (EB) [15]. In this work we have studied the influence of a minor groove binding probe, hoechst 33258 (HOE), on the DNA torsional dynamics by the same technique and have compared it with the effects reported for the intercalator chloroquine [16,17] by looking at the ethidium fluorescence polarisation anisotropy decay. After a short summary of the theory of FPA, we trace a parallel between the usual time domain approach, corresponding to short pulse excitation, and the more recent frequency domain technique employed in FPA, pointing out, with the aid of computer simulations, how changes in the parameters associated with DNA torsional motions, affect the results. The influence of a second intercalator, chloroquine, on the dynamics of nucleic acid–EB complexes has been shown with frequency domain FPA measurements on both a linear standard DNA and covalently closed circular DNAs. The effect of a ligand that binds to DNA in the minor groove, hoechst 33258, has been studied and a comparison between the results is given in the discussion.

## 2. Torsional dynamics

DNA in solution is subjected to Brownian forces due to thermal excitation. Essentially two types of low frequencies molecular motions occur: torsional motions of the base pairs along the helix axis and bending motions perpendicular to the helix axis. So far these motions have been described analytically by models that consider torsion and bending as completely uncoupled [12–14] and give a description of the dynamics by means of few measurable parameters. Due to the length of the DNA samples studied in this research, the two motions occur on different time scales and, by employing the DNA–EB complex, only the torsional motions are accessible with FPA experiments.

Two models which predict these motions have been developed: the model of Barkley–Zimm [13] and the model of Schurr [12,14]. We have chosen to use the latter since it is based on a more general formalism. The dye can bind at each site on DNA, and the dye dipole coordinates have been expressed by Eulerian angles that were not restricted to small angle limits. Since the details of the formalism are given in the cited papers, we recall here only the expression used for data analysis.

The fluorescence anisotropy time decay can be written as a sum of five terms, and, if we neglect the rapid wobbling motions of the dye inside the intercalation pocket, each term is factorized in the product of three correlation functions:

$$r(t) = r_0 \sum_{n=-2}^{2} I_n(t) F_n(t) C_n(t) \qquad (1)$$

(a) $I_n(t)$ is the internal correlation function. If we consider the probe as tightly bound to DNA, these terms are simply trigonometric expressions of the angle

formed by the EB dipole and the helix axis: $\epsilon = 70.5°$ [18]. For the case examined here by neglecting the first early times under one nanosecond of the EB decay (EB lifetime is about 22.5 ns), one removes the contribution of EB wobbling to FPA. This causes the limiting anisotropy value, $r_0$, to be as low as 0.36 instead of 0.4, as one should find for the case of parallel absorption and emission dipoles [19].

(b) $F_n(t)$ is the bending correlation function. Recently a correct expression for $F_n(t)$ has been derived for DNA chains as long as $L/P \leqslant 0.6$, where $P$ is the DNA persistence length [20], corresponding to DNA shorter than 200 base pairs. For DNA of this length bending and torsional motions occur in the same time range, while for much longer DNAs, ($L \approx 2000$ b.p.), it is reasonable to assume that the helix axis remains practically fixed during torsional motions. This would correspond to an infinite persistence length of DNA. In any case, the elastic constant value estimated according to the above assumption is a lower bound of the actual value since the finite axis length of DNA helix [21,19]. In this work we always assume $F_n(t) = 1$.

(c) $C_n(t)$ is the torsional correlation function. The complete expression is found in reference [12], but when considering the kind of probe used here and the length of our DNA samples, we can use the so called 'intermediate zone formula', which describes exactly the torsional decay:

$$C_n(t) = \exp(-n^2\sqrt{t/\xi}), \text{ where } n = 0,1,2$$

and

$$\xi = \frac{\pi\alpha\gamma}{k_B^2 T^2} \tag{2}$$

$\xi$ has the dimensions of a time (here called 'characteristic time') and it is by far the most interesting parameter since it is the product of $\alpha$, the elastic constant, and $\gamma$, the rotational friction coefficient. Typical values of $\alpha$ range from 3 to $7 \times 10^{-12}$ erg; $\gamma$ depends on temperature, solvent viscosity ($\eta$) and DNA radius (R) through the law:

$$\gamma = 4\pi R^2 h \eta, \tag{3}$$

where $h$ is the height of the cylinder formed by one base pair whose value is assumed to be $3.4 \times 10^{-8}$ cm; $\gamma$ has been measured by Wu et al. [22], and found $\gamma = 6.15 \times 10^{-23}$ erg × s at 20° C, which corresponds to $R = 12$ Å if $h = 3.4 \times 10^{-8}$cm, (Eq. 3). The elastic constant can be related to the fourth power of DNA radius through the moment of inertia ($I = m(R^2)R^2$) of a cylindrical cross section per unit height $h$:

$$\alpha = E(1+\sigma)I/h, \tag{4}$$

where $\sigma$ is the well known Poisson ratio [13] which relates the elastic constant $\alpha$ to the Young modulus $E$.

The complete expression used when describing data concerning brownian anisotropy is given by:

$$r_b(t) = r_0[I_0 + I_1 \exp(-\sqrt{t/\xi}) + I_2 \exp(-4\sqrt{t/\xi})], \tag{5}$$

where the trigonometric factors are written as: $I_0 = \frac{1}{4}[3\cos^2\epsilon - 1]^2$; $I_1 = 3\sin^2\epsilon\cos^2\epsilon$ and $I_2 = 3/4 \sin^4\epsilon$.

## 3. FPA in $\tau$ and in $\omega$: a comparison

In the time domain FPA, the quantities that are usually measured are the components of the fluorescence intensity parallel and perpendicular to the directions of the pulsed excitation beam polarisation. These quantities, named $I_\parallel$ and $I\perp$, respectively, are linear in the fluorescence anisotropy $r$:

$$I_\parallel(t) = I(t)\left(\frac{1+2r(t)}{3}\right),\ I_\perp(t) = I(t)\left(\frac{1-r(t)}{3}\right). \tag{6}$$

In the frequency domain, instead, one measures the difference between the phase angles $\Delta$ of the two components with respect to the (modulated) excitation beam and the corresponding demodulation ratio $\Lambda$ defined as:

$$\Delta(\omega) = \phi_\perp(\omega) - \phi_\parallel(\omega),\ \Lambda(\omega) = \frac{M_\perp(\omega)}{M_\parallel(\omega)}. \tag{7}$$

These experimental quantities are related to the anisotropy decay in the time domain by means of Laplace transforms ($L_\omega$) of the two components of the fluorescence intensity $J_i(\omega) = L_\omega[I_i(t)]$ [23] where the subscript '$i$' indicates either $\parallel$ or $\perp$:

$$\Delta^c(\omega) = \text{arctg}\left(\frac{\text{Im}(J_\perp)\text{Re}(J_\parallel) - \text{Re}(J_\perp)\text{Im}(J_\parallel)}{\text{Re}(J_\perp)\text{Re}(J_\parallel) + \text{Im}(J_\perp)\text{Im}(J_\parallel)}\right),$$

$$\Lambda^c(\omega) = \frac{|J_\perp|}{|J_\parallel|}. \tag{8}$$

From a theoretical prediction of $r(t)$, one can obtain the expected values of phase angle difference and demodulation ratio. In particular as we saw in the preceding paragraph, for the DNA–EB complex the expression for the fluorescence anisotropy decay is given by the intermediate zone formula (5). In many instances, due to uncompleted binding, it is also necessary to take into account the free dye contribution to the signal and, consequently, the measured anisotropy of the mixture of bound and free dye is given by [24]:

$$r(t)=\frac{x_b e^{-\Gamma_b t} r_b(t)+x_f e^{-\Gamma_f t} r_f(t)}{x_b e^{-\Gamma_b t}+x_f e^{-\Gamma_f t}}, \qquad (9)$$

where $\Gamma_{b,f}$ are the decay rates of the bound and the free dye, $x_{b,f}$ are the pre-exponential factors for the two species, $r_b(t)$ is the brownian anisotropy of bound EB and $r_f(t)$ represents the free dye rotational contribution. The details of the procedure leading to $\Delta(\omega)$ and $\Lambda(\omega)$ have been given elsewhere [15].

The experimental data have been analysed by means of a non-linear least squares program by minimisation of the reduced chi-square function by means of the Marquardt algorithm:

$$\chi_R^2=f^{-1}\sum_{\omega}[(\Delta_\omega-\Delta_\omega^c)/\sigma_\Delta]^2 + f^{-1}\sum_{\omega}[(\Lambda_\omega-\Lambda_\omega^c)/\sigma_\Lambda]^2. \qquad (10)$$

Here $f$ indicates the number of degrees of freedom and $\sigma_\Delta$ and $\sigma_\Lambda$ are the estimated experimental uncertainties affecting the measured quantities. As the phase and the modulation measurements are two independent measures, the number of experimental data is twice the number of modulation frequencies chosen.

The behaviour of phase differences and demodulation versus $\omega$ is determined by the three parameters $\xi$, $r_0$ and $x_f$. The quantity of major interest, $\xi$, defined in Eq. (2), is related to the torsional constant of DNA $\alpha$ and to the friction coefficient $\gamma$. The limiting anisotropy of EB, $r_0$, has been previously introduced (Eq. (1)). The free dye fractional intensity, $a_f$, is related to the free dye lifetime and to its pre-exponential factor $x_f$. It is helpful to produce simulations when changing one parameter at a time and to compare these frequency domain simulations with the corresponding curves in the time domain in order to show the sensitivity of the technique to the above parameters. These simulations, previously shown for proteins and membranes at different values of the relevant parameters such as correlation times and their weights [25–27], are given here for the DNA–EB complex fluorescence modulation. In all the simulations it is assumed that the temperature is 20°C and the rotational friction factor has the value $\gamma=6.15\times10^{-23}$ erg×s.

In Fig. 1 one can see the influence of the time decay of the probe on the phase angles differences (i.e. its FPA). To be noted that in the time domain, the lifetime $\tau$ of the probe limits the useful time range of the anisotropy investigation to a few lifetimes, whereas in the frequency domain the fluorescence modulation ratio depends on the probe lifetime and sets an upper limit for the highest frequencies suitable for anisotropy measurements. Furthermore, while in the time domain the fluorescence anisotropy $r(t)$ does not depend on the probe lifetime (it is a ratio of intensities) [24], in the frequency domain, on the other hand, we use phase angle differences and demodulation ratios that are both influenced by the probe lifetime. This situation is shown in Fig. 1: in the inset the modulation value (i.e. total intensity measurements) for three hypothetical lifetime of 2 ns, 22.5 ns (the actual value for EB) and 100 ns are shown while in the main figure are considered the phase angle differences obtained by a simulated anisotropy measurement of a DNA–dye complex

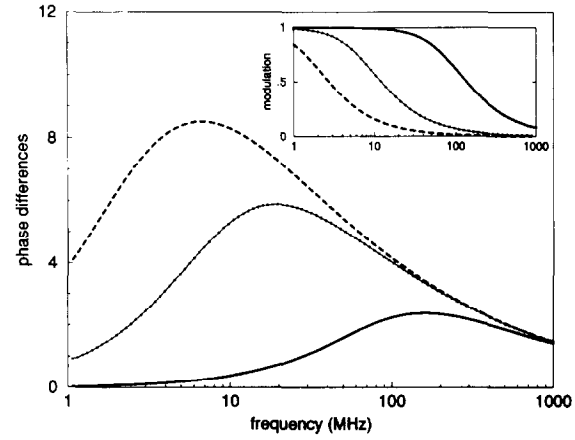


Fig. 1. Simulation of FPA phase difference versus modulation frequency of a dye–DNA complex. The lifetimes of the hypothetical probes are 2 ns decay (solid line), 22.5 ns decay (circles) and 100 ns decay (dashed line); the elastic torsional constant of DNA is $\alpha=5\times10^{-12}$ erg, the limiting anisotropy is $r_0=0.36$, and the probe fractional intensity is zero. Fluorescence modulation is shown in the inset.

with the anisotropy decay given in Eq. (5). Here we have assumed that all the probes are bound to DNA ($a_f=0$), the limiting anisotropy has been set at $r_0=0.36$ [19] and the torsional constant has been kept at $\alpha=5\times10^{-12}$ erg. We note that EB has very favourable properties since its modulation is still high in a frequency range where most of the information of FPA is falling. Data have been collected up to a frequencies where the modulation is about 20% of the initial (largest) value in order to keep noise effects to a minimum. For a 22.5 ns lifetime, this top frequency is about at 40 MHz, but its value would fall to 8 MHz for a hypothetical 100 ns decay. On the contrary, with 2 ns lifetime, typical of many aromatic dyes, the upper useful frequency would increase to 400 MHz. The last case, however, would not show a significant variation in the phase angle difference, and, consequently, the measurements display little sensitivity on the parameters.

The next step has been that of simulating the curves while changing the parameters $r_0$, $a_f$ and $\alpha$ for both time and frequency domain focusing on time ranges (1 to 100 ns) and frequency ranges (1 to 100 MHz) explored during a typical measurement. For the free dye decay the value of 1.7 ns has been used as obtained by measurements of EB in buffer solution. When changing the values of the limiting anisotropy $r_0$, a simple translation of the modulation ratios and a progressive decrease in phase angle differences occurs (data not shown). On the contrary, large effects are found when the free dye fractional intensity $a_f$ varies by only a few percent. In the time domain the free dye contribution occurs only at early times, as shown in Fig. 2a, and therefore, when missing the first nanoseconds of the decay, the free dye contribution is no longer detectable with sufficient accuracy. If not interested in the free dye contribution, it is then sufficient to neglect these early times decay in the time domain, but things are different in the frequency domain (Fig. 3a), where mixing of the frequencies is caused by the Laplace transform of the intensity necessary to go from the time to the frequency domain. Here, in fact, the free dye presence causes negative values of the phase angle differences and an increase in the demodulation ratios at the high frequency extreme. This situation generally occurs in the frequency domain anytime two distinct rotating species are both present in solution and it is an unequivocal behaviour.

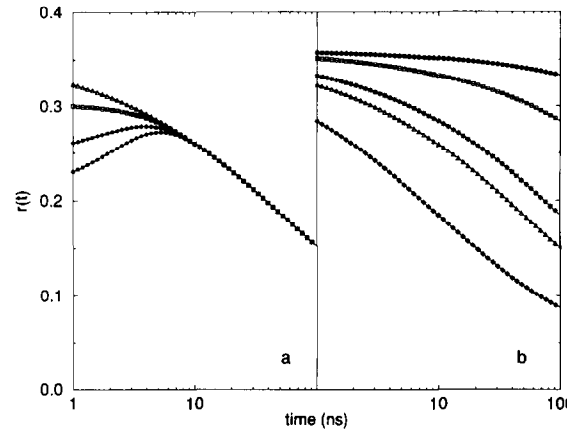


Fig. 2. Time domain simulations of fluorescence anisotropy decay of DNA–EB complex. (a) Simulations with $\alpha=5\times10^{-12}$ erg and $r_0=0.36$ at different free dye fractional fluorescence intensities: (△) $a_f=0$; (□) $a_f=0.01$; (*) $a_f=0.03$; (●) $a_f=0.05$. (b) Simulations with $r_0=0.36$ and $a_f=0$ at different values of DNA elastic constant constant: (◆) $\alpha=10^{-12}$ erg; (△) $\alpha=5\times10^{-12}$ erg; (*) $\alpha=10^{-11}$ erg; (□) $\alpha=10^{-10}$ erg; (●) $\alpha=10^{-9}$ erg.

In Figs. 2b and 3b simulations are shown versus the torsional constant, varying from the value of $10^{-12}$ erg up to $10^{-9}$ erg. This is equivalent to vary the torsional time $\xi$ from $10^{-7}$ s to $10^{-4}$ s and, since the torsional time is proportional to the product of the torsional constant and of the rotational friction coefficient, these simulations would represent as well a variation of $\gamma$ from $10^{-23}$ erg×s to $10^{-19}$ erg×s if a fixed value of $\alpha=5\times10^{-12}$ erg is chosen. In the time domain (Fig. 2b) the behaviour of $r(t)$ becomes nearly time independent at increasing torsional rigidities. The curves in the frequency domain (Fig. 3b) are very sensitive to the value of the torsional constant for less than $100\times10^{-12}$ erg, but they become almost frequency independent as the value of $\alpha$ increases. This is consistent with the fact that when DNA becomes more rigid, then less depolarisation can occur during the dye lifetime. As seen from the above simulations, the frequency domain curves are strongly affected by variations of the parameters discussed and, even at first glance, it is often possible to infer how each parameter is contributing to the data.

## 4. Materials and methods

### *4.1. Sample preparation*

Calf thymus DNA (CT) was purchased from Sigma Chemical Co. and used without further purification.

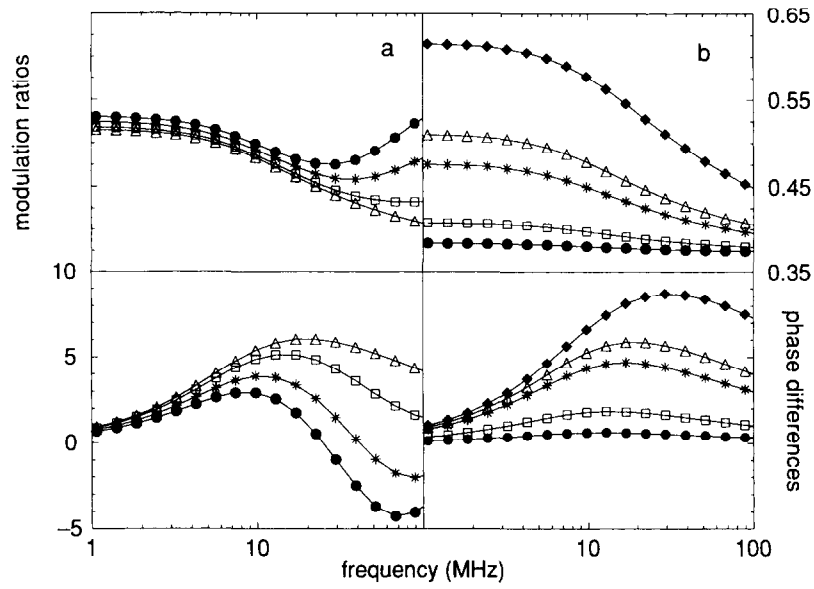


Fig. 3. Frequency domain simulations of fluorescence anisotropy decay of DNA–EB complex; modulation ratios are shown in the upper section and phase angle differences in the lower section. (a) Simulations with $\alpha = 5 \times 10^{-12}$ erg and $r_0 = 0.36$ at different free dye fractional fluorescence intensities: (△) $a_f = 0$; (□) $a_f = 0.01$; ( * ) $a_f = 0.03$; (●) $a_f = 0.05$. (b) Simulations with $r_0 = 0.36$ and $a_f = 0$ at different values of DNA elastic constant constant: (◆) $\alpha = 10^{-12}$ erg; (△) $\alpha = 5 \times 10^{-12}$ erg; ( * ) $\alpha = 10^{-11}$ erg; (□) $\alpha = 10^{-10}$ erg; (●) $\alpha = 10^{-9}$ erg.

The plasmids DNA were derived from pUC18m (2686 base pairs) and throughout this work they are indicated as P2 (2912 b.p.) and P6 (3364 b.p.) [28]. Plasmids replication was obtained by harbouring in *E.Coli* HB101 and prepared by lisozyme/SDS lysis and polyethylene-glycol precipitation. DNA was then purified by HPLC and checked on agarose gel electrophoresis.

DNA samples were dissolved in phosphate buffer (10 mM $KH_0PO_4$, 30 mM $Na_2HPO_4$, 0.1 mM $Na_3$-EDTA; pH = 7.5, ionic strength $I = 100$ mM) some days before each measurement and maintained at 4°C. For the molar extinction coefficient at 258 nm the same value was taken for all DNA samples: $\epsilon^{258} = 6600\ M^{-1}\ cm^{-1}$.

Ethidium bromide (EB) and chloroquine (CQ) were also purchased from Sigma Chemical Co., hoechst 33258 (HOE) was purchased by Aldrich Chemie. All the dye were dissolved in water and the stock solutions were stored at dark at 4°C. The molar extinction coefficients used for determining dye stock concentrations with a standard spectrophotometer are the following: $\epsilon^{478} = 5860\ M^{-1}\ cm^{-1}$ for EB, $\epsilon^{338} = 42000\ M^{-1}\ cm^{-1}$ for HOE and $\epsilon^{343} = 19000\ M^{-1}\ cm^{-1}$ for CQ.

All the dyes were added to solutions of DNA of known concentration ( ≅ 100 μM) just before each measurement; the little additions of dyes stock solutions were weighted accurately in order to know dye concentration in solution. The ionic strength was maintained constant by adding NaCl to dye stocks. Care was used with hoechst 33258 additions as DNA precipitation could occur if the dye stock was much too concentrated.

### 4.2. Instrumentation

A frequency domain fluorometer (K2, I.S.S. Urbana, ILL, USA) has been used for anisotropy and lifetime measurements. The details on this technique can be found in the literature (see, for example, ref. [29]). As light source, a horizontally polarised beam of an Argon laser (2025/5 Spectra Physics) tuned on the green line at 514 nm was used, with a power output of 500–700 mW. The beam enters a double Pockels cell through a two-way polariser. A radio frequency, ranging from 0.6 MHz to 300 MHz, is applied to the cell and modulates the light beam intensity (40–70% of modulation). The excitation beam is vertically polarised and the fluorescence signal emitted at 90° is analysed through a long pass filter (550 nm), a second polariser, and is detected by a R928 Hamamatsu photomultiplier tube. The time behaviour of the intensity

of the excitation beam is detected before the sample compartment by a reference PMT.

The acquisition unit detects the DC and the AC parts of the current coming either from the sample PMT ($AC^S$, $DC^S$) and from the reference PMT ($AC^0$, $DC^0$). The absolute phase delay $\phi$ is measured as $\phi = (\phi_0 - \phi_S) - (\phi_0 - \phi_R)$, where '0' refers to the incident light, 'S' to the fluorescence light from the sample and 'R' to the fluorescence light from a reference sample of known lifetime. The absolute modulation is given by the ratio: $M = (AC/DC)_S/(AC/DC)_R$.

For anisotropy measurements, the emission polariser is rotated alternatively from the vertical (parallel to the excitation) to the perpendicular position. For each step, the modulation and the phase values are taken and combined to give the difference phase delay $\Delta = \phi_\perp - \phi_\parallel$, and the modulation ratio $\Lambda = M_\perp / M_\parallel$. A personal computer directly drives the polarisers, the shutters and the sample turret, and sets the two synthesisers to the appropriate modulation frequency. It also acquires the data that are next visually examined and fitted by means of an HP Apollo 9710 workstation.

During anisotropy measurements 20 logaritmically spaced frequencies are used ranging from 1 MHz to 40 MHz while for lifetimes measurements 15 frequencies are usually taken; the phase and modulation uncertainties are respectively $\sigma_\Delta = 0.2°$ and $\sigma_\Lambda = 0.004$.

All the measurements were done keeping the temperature constant at a known value (23°C) by means of a Haake termostating bath. Temperature was measured by introducing a thermocouple in the reference sample.

## 5. Results

Fluorescence lifetimes and FPA of EB have been measured both in linear CT DNA and in two plasmids (P2 and P6) of different superhelical density ($\pm 2$ superhelical turns). DNA motions have been investigated by measuring the signal from intercalated EB, one molecule per 200 base pairs, approximately. Two different 'perturbing' probes, chloroquine and hoechst 33258, have been added to the solutions.

All the results presented here are fitted with the intermediate zone expression (Eq. (2)) which gives the torsional time $\xi$ that is related to the product of the elastic constant $\alpha$ and the friction factor $\gamma$. The figures display the values of the elastic constant obtained from Eq. (2) at fixed $R$, labelled $\alpha^*$, an effective value of $\alpha$ since it includes the effects of boundary constraints and ligand saturation. At vanishing binding and in the absence of boundary constraints, $\alpha^*$ should become indistinguishable from $\alpha$.

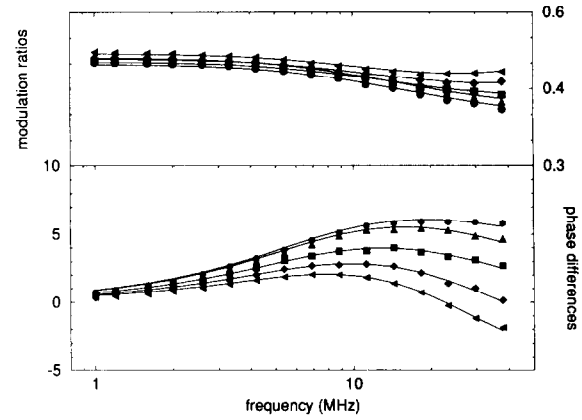


Fig. 4. Anisotropy measurements of CT–EB complex at increasing chloroquine/base pair ([CQ]/[BP]) concentration. Modulation ratios are shown in the upper section and phase angle differences in the lower section. (●) [CQ]/[BP] = 0; (▲) [CQ]/[BP] = 8.5; (■) [CQ]/[BP] = 19.3; (♦) [CQ]/[BP] = 39.7; (◀) [CQ]/[BP] = 57.7. Solid lines represent fittings to experimental data.

### 5.1. Intercalator saturation

In Fig. 4 data on EB FPA are presented vs. increasing chloroquine (CQ) concentration bound to CT DNA. The largest concentration is equivalent to about 50 CQ per base pair. Data for the plasmids investigated have a similar behaviour. By fitting the data with Eq. (9) one can obtain the three parameters of interest: the torsional time $\xi$, the free dye fractional intensity, $a_f$ and the limiting anisotropy $r_0$. It has been found that $a_f$ increases up to 0.04 for linear DNA and to 0.057 for the two plasmids, yielding characteristic negative values for the phase angle differences (Fig. 4). The value of this parameter was confirmed by measuring the EB lifetime at each chloroquine concentration. $r_0$ was found close to 0.37, in the absence of intercalated chloroquine, but values down to 0.32 at the largest CQ saturation were also found. The torsional properties of the 'unperturbed' (low dye/BP) plasmids reveal a small difference that might be out of the experimental error, $\alpha = (4.9 \pm 0.12) \times 10^{-12}$ erg for P2 and

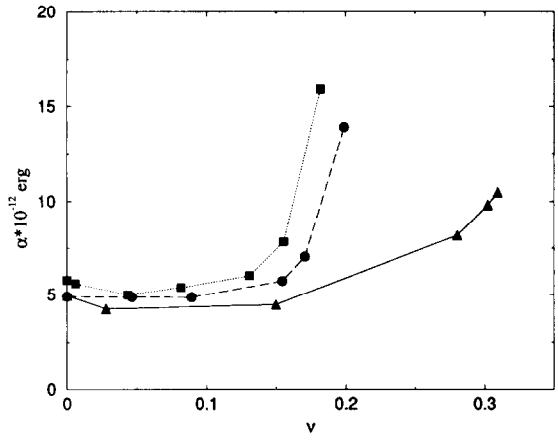


Fig. 5. Effective elastic constant $\alpha^*$ versus chloroquine bound to DNA, $\nu = [CQ]^{bound}/[BP]$: (▲) Calf Thymus; (●) P2 plasmid (■) P6 plasmid.

$\alpha = (5.6 \pm 0.2) \times 10^{-12}$ erg for P6, while $\alpha = (5.2 \pm 0.2) \times 10^{-12}$ erg for CT DNA. Here it is unnecessary to distinguish between $\alpha$ and $\alpha^*$ due to the little concentration of EB used to measure the elastic constant as will be discussed later. In Fig. 5 $\alpha^*$ is plotted versus bound chloroquine per base pair concentration, $\nu$, evaluated according to the estimated the association constant [30,16] under the same ionic strength condition. For linear DNA, apart from an initial slight decrease, the effective elastic constant remains constant up to $\nu = 0.14$–$0.16$, then there occurs a twofold increase at the highest binding ratio investigated. For the two plasmids, $\alpha^*$ stays constant up to $\nu = 0.14$, then there follows an increase steeper than that observed in the linear case, probably due to the topological constraints of a circularly closed DNA.

### 5.2. *Role of outer binding: hoechst 33258*

DNA has been perturbed with a second type of ligand: hoechst 33258, a well known minor groove binder, often used for in vivo cytological stain of chromosomes, since it is highly fluorescent [31–34]. Here HOE has been used in order to induce a conformational perturbation and, when exciting EB at 514 nm, the groove binder is silent just as it occurs with chloroquine.

FPA of the EB–DNA complex has been evaluated at increasing HOE concentrations either in linear DNAs or in different closed circular DNAs. In Fig. 6 differential phase angles and demodulation ratios are shown for CT DNA: similar data are obtained for the circular DNA samples. The trend in demodulation data at increasing HOE concentration looks different from the CQ case. In fact, at increasing chloroquine concentration, modulation values increase, while the opposite occurs at increasing HOE concentration until an almost constant behaviour is obtained (except at the high frequency limit, where free dye contribution is important). Also phase data appear different in the two cases. With the exception of a common increase of the free dye contribution with dye (CQ or HOE) concentration, phase differences data approach constant values with frequency for HOE instead of showing a maximum as for CQ data. It is useful to compare these two cases with the simulations showed in the frequency domain in Fig. 3. The chloroquine case is closer to the simulation of Fig. 3a in which the free dye contribution is varied, while the hoechst data appear as a superposition of two effects: a change of the free dye amount (Fig. 3a) and a change of the characteristic time $\xi$ (flat phase and modulation curves) (Fig. 3b). In fact, when fitting HOE data with Eq. (9), a large increase in $\xi$ is found.

A behaviour of phase angles differences and modulation ratios similar to that obtained with HOE and shown in the Fig. 6, can also be derived in a very different situation: by varying the solution viscosity with the addition of increasing concentration of glycerol to a DNA–EB solution. These viscosity measurements show an increase in the characteristic time $\xi$

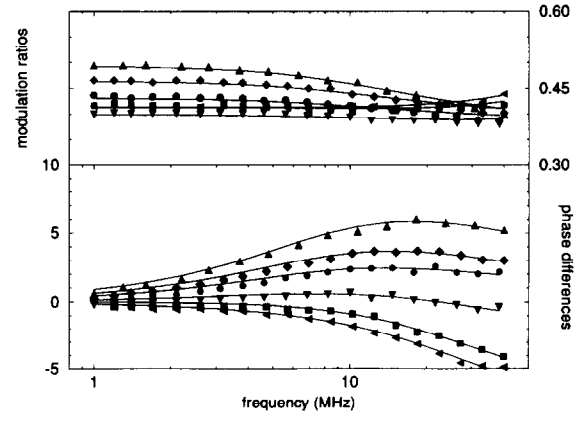


Fig. 6. Anisotropy of CT–EB complex at increasing hoechst 33258/base pair concentration ([H]/[BP]). Modulation ratios are shown in the upper section and phase angle differences in the lower section: (▲) [H]/[BP] = 0; (◆) [H]/[BP] = 0.47; (●) [H]/[BP] = 0.6; (▼) [H]/[BP] = 0.75; (■) [H]/[BP] = 0.9; (◀) [H]/[BP] = 1. Solid lines represent fittings to experimental data.

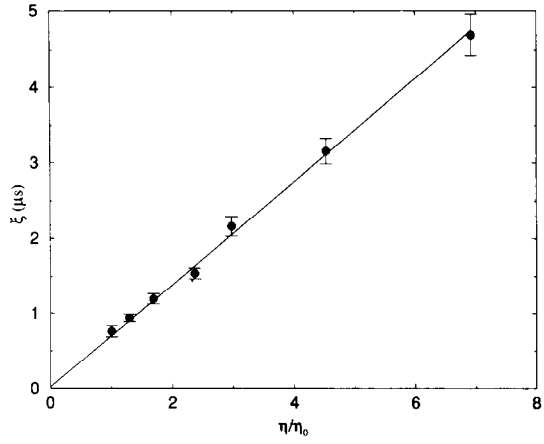


Fig. 7. Characteristic time $\xi$ versus relative solution viscosity $\eta/\eta_0$: experimental data (●) and interpolating linear regression fit.

together with an increase of the free dye concentration due to the lower association constant of EB in the presence of glycerol (data not shown).

## 6. Discussion

The above reported data indicate that frequency-modulated FPA is a suitable technique for studying the torsional characteristics of DNA under a variety of perturbations. From theoretical analysis one finds that two factors are involved in the exponentials describing the fluorescence anisotropy decay: the elastic constant $\alpha$ and the rotational friction factor $\gamma$. In particular $\alpha$ can be determined if $\gamma$ is estimated from Eq. (3) and from known values of helix radius and pitch together with the solution viscosity. The dependence of $\gamma$ upon viscosity has been tested as shown in Fig. 7 where a linear relationship between the characteristic time $\xi$ (Eq. 2) and viscosity is obtained thereby supporting the validity of Eq. 3 and suggesting the independence of elastic constant upon solution viscosity.

Before discussing the results of FPA decay in the presence of saturating probes we recall:

(1) EB is added to DNA samples at very low concentration in order to avoid EB–EB interactions such as Förster energy transfer which would affect FPA [15].

(2) Chloroquine is an intercalator of DNA that does not respond to light excitation at $\lambda = 514$ nm thus leaving the fluorescence emission only to EB.

(3) Hoechst 33258 is a molecule that interacts with DNA by wrapping mainly in the minor groove and again HOE does not respond to EB excitation at $\lambda = 514$ nm.

Before discussing the different ligands a word of caution should be given. Fits of FPA data with the intermediate zone expression [14] are generally successful as can be seen in the Figs. 4 and 6. In some cases, at ligand saturation, the elastic constant values are found extremely large. However, changes in the torsional constant could be due also to the presence of boundary constraints and other perturbations as it will be discussed later, and therefore the value of the elastic constant which describes the data will be defined as an effective torsional constant and labelled $\alpha^*$.

### 6.1. Chloroquine saturation data

It has already been pointed out that at high chloroquine binding ratios, a substantial release of EB versus CQ intercalation occurs with consequent changes in phase angle differences and demodulation ratios (Fig. 4). From the $\alpha^*$ values obtained when fitting the data (Fig. 5) one notices their almost constant behaviour up to a binding ratio value of $\nu \cong 0.14$, corresponding to about one chloroquine every 7 base pairs and equivalent to an average distance between intercalated CQ of about 24 Å. Then, for linear DNA, it follows a smooth increase corresponding to the doubling of $\alpha^*$ at the highest binding ratio investigated $\nu = 0.32$ (1 dye every 3 b.p.).

For circularly closed DNA the behaviour is slightly different: a sharper increase has been recorded for binding ratios above the value known as 'critical $\nu$', i.e. the intercalator binding ratio necessary to release the superhelical turns and to put DNA in a relaxed conformation. The $\alpha^*$ increase at the highest chloroquine binding ratio investigated, is about threefold. This result is not unexpected since the topological constraints induce an additional elastic torsional term when filling up a covalently closed DNA with an intercalating dye. Whilst in linear DNA this contribution can be released, in circular closed DNA, on the other hand, torsional stress is built up to the point where the torsional dynamics is modified.

Since these effects are meaningful only at pronounced dye binding ratios, we can safely assume that the small dye concentration employed in order to meas-

ure FPA, 1 EB per 200 base pairs, corresponding to average dye to dye distances of about 70 nm, does not alter appreciably the dynamical properties of the host DNA. In particular, it appears that several intercalating dyes per 'wavelength' of torsional motions (ranging from 18 nm to 100 nm [14]) are required in order to induce significant alterations of the torsional dynamics, in agreement with the observed effects that show up only when dye to dye distances are shorter than one helix turn (3.4 nm).

In the above discussion the torsional time constant $\xi$ has been attributed to a change of $\alpha$ through the elastic modulus $E$ (Eq. (4)), although a change of the DNA radius should be considered. According to Eq. (3) $\gamma$ depends upon the square of the DNA radius $R$, while $\alpha$ is proportional to its fourth power and therefore $\xi$ is related to the sixth power of $R$. A threefold increase in $\alpha^*$ would then require a 20% change in DNA radius i.e. a 44% mass increase. Since the highest investigated [CQ]/[BP] ratio corresponds to 50 chloroquines per base pair, an external binding of a chloroquine molecule every two base pairs, necessary to justify the threefold increase in $\alpha^*$, cannot be excluded.

### 6.2. *Hoechst 33258 saturation data.*

The HOE data, Fig. 6, can also be successfully fitted with the same intermediate zone formula (Eq. (5)), previously used for chloroquine binding and viscosity measurements and the value of an effective elastic constant $\alpha^*$ can be obtained.

In Fig. 8 $\log(\alpha^*)$ values, derived from the best fit, at constant R, are presented versus the [H]/[BP] ratio, where [H] and [BP] are the total HOE and DNA base pair concentrations in solution. Linear DNA and plasmids appear to display the same behaviour, as can be seen in the figure where CT DNA is reported together with plasmid P6. The feature of this plot is the dramatic increase of $\alpha^*$ corresponding to more than five orders of magnitude. The [H]/[BP] axis can be quite naturally separated in two regions. At low [H]/[BP] values, up to [H]/[BP] $\approx 0.5$, $\log \alpha^*$ is linear versus HOE mole fraction. At [H]/[BP] $\approx 0.5$ a threefold increase of $\alpha^*$ is found, close to the largest change of $\alpha^*$ found for chloroquine. In the range $0.5 \leqslant$ [H]/[BP] $\leqslant 1.2$, $\alpha^*$ increases more than four orders of magnitude. At the same time the free EB fractional intensity $a_f$, vanishingly small up to [H]/[BP] $\approx 0.5$, rises to

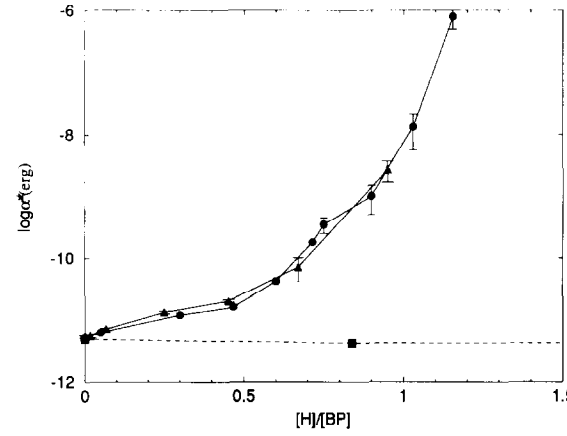


Fig. 8. Logarithm of the effective elastic constant $\alpha^*$ versus [H]/[BP]: (●) Calf Thymus; (▲) P6 plasmid; (■) [CQ]/[BP] data for CT DNA are shown for comparison.

$a_f = 0.045$ at the highest HOE concentration. The value [H]/[BP] $\approx 0.5$ corresponds to the onset of unspecific HOE binding reported by Lootiens et al. [35]. HOE is known to display a few binding modes to DNA which have been characterised in term of their stoichiometry [35] but the association constant has been measured only for the primary specific binding in the minor groove [35,36]. HOE is believed to bind specifically to runs of four A–T in the minor groove [37] up to [H]/[BP] $\approx 0.5$. This binding mode has the strongest association constant ($K \approx 10^9\ M^{-1}$), while the affinity decreases for binding sites having different base pairs composition [37].

Several mechanisms can be considered in order to describe the large values of $\alpha^*$. In order to compare experimental data with expected behaviour, it has been found convenient to simulate 'data' corresponding to the best fit values of the FPA parameters in the absence of free dye. The simulations are shown in Fig. 9a.

(1) *Change in DNA radius.* The $10^4$ to $10^6$ fold increase of $\xi \approx \alpha\gamma$ according to Eq. (2), if tentatively attributed only to a change of $R$, would require to a 5 to 10 fold increase of the DNA radius since $\xi \approx R^6$ according to Eq. (4). It appears difficult to justify even the lower radius increase upon HOE binding since the largest amount of dye in solution ([H]/[BP] $\approx 1$), if condensed on DNA, would yield at most 20% and therefore effects due to changing $R$ would account only for a threefold increase of $\alpha^*$.

(2) *Aggregation.* Suppression of internal motions does not seem to be due to DNA macroscopic aggre-

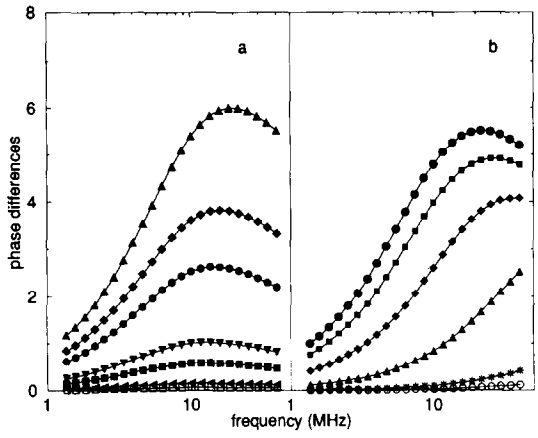


Fig. 9. (a) Simulated 'experimental data' without free EB contribution. (▲) [H]/[BP] = 0; (♦) [H]/[BP] = 0.47; (●) [H]/[BP] = 0.6; (▼) [H]/[BP] = 0.75; (■) [H]/[BP] = 0.9; (▶) [H]/[BP] = 1; (□) [H]/[BP] = 1.15. (b) Simulated data with $\alpha = 5 \times 10^{-12}$ erg and $r_0 = 0.36$ for a clamped DNA of different length: (●) 500 BP, (■) 200 BP, (♦) 100 BP, (▲) 50 BP, (*) 20 BP, (○) 10 BP.

gates or precipitation induced by HOE binding, contrary to what reported by Comings [38], as confirmed also by static light scattering observations. In fact, during the measurements, which lasted 5 h, no trace of precipitation was found, even at the highest concentration investigated, nor evidence of precipitation was reported by Lootiens et al [35].

(3) *EB binding geometry.* The EB binding site might be distorted by the presence of HOE molecules bound nearby. A change of binding site geometry could result in an apparent increase of the torsional constant $\alpha$. For these reasons some frequency domain FPA simulations were done on the EB–DNA complex with fixed values of the limiting anisotropy $r_0 = 0.36$ and of the elastic constant, $\alpha = 5 \times 10^{-12}$ erg, while changing $\epsilon$, the angle that the EB dipoles form with the helix axis, from the known value $\epsilon = 70.5°$ [18] to 50° and 30°. The simulated phase differences and modulations follow the behaviour of the experimental data, with both phase differences and modulation ratios decreasing as $\epsilon$ becomes smaller (data not shown). Yet at $\epsilon = 30°$ degrees, however, phase and modulation curves are not as flat as those found at the highest HOE concentrations. It should be added that, such a deformation in the binding site geometry would practically exclude EB intercalation and a change in the lifetime of bound EB should occur. This is not observed.

(4) *EB binding at HOE site.* EB might bind in the DNA region where HOE is already bound. In this case its response would not represent the overall of the DNA chain dynamics, but a localised perturbation. Since HOE binds as a ribbon in the minor groove, it probably locks 4 or 5 base pairs and locally the elastic constant is greatly enhanced. If a greater number of EB molecules were bound at the base pairs occupied by or next to a HOE molecule, an increase of the measured torsional constant should be expected. This situation, however, does not seem to occur since EB is released at increasing HOE concentration (Fig. 6). From EB Scatchard plots in the presence of HOE it has been previously found (unpublished results) that the number of sites for EB is reduced by the number of sites occupied by HOE: this supports the idea that EB is not likely to bind the sites already occupied by HOE.

(5) *Clamped ends DNA.* The large perturbation of the overall DNA dynamics induced by HOE as shown by $\alpha^*$ in Fig. 8 must be considered. Binding of HOE to the DNA minor groove along 4–5 adjacent base pairs appears then to hinder DNA torsional motions. It seems unlikely, however, that the elastic constant of DNA could reach the extreme values given in Fig. 8. We rather feel that $\alpha^*$ reflects the influence of boundary conditions such as those created by large amounts of HOE at some points, see, e.g., Fig. 10. We may assume that the DNA segments heavily loaded with HOE are nearly fixed at their extremes and, in order to simulate FPA, we describe the torsions with 'clamped ends' [14]. Simulations of the frequency domain FPA, while varying the length of the clamped chain and keeping $\alpha = 5 \times 10^{-12}$ erg and $r_0 = 0.36$, show a behaviour that is in qualitative accordance with the experimental data obtained with HOE. Both phase differences and mod-

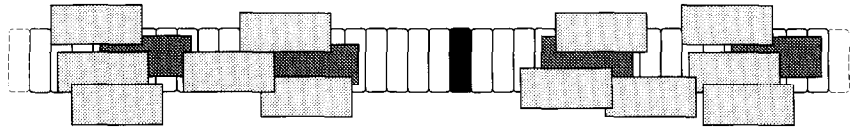

Fig. 10. Schematic representation of DNA covered with HOE at saturating level: the black disk represents EB. HOE molecules bound in the primary binding mode, i.e. wrapping in the minor groove, are shown in dark grey, while external bound HOE are the lighter rectangles.

ulation ratios decrease when shortening the clamped tract, but the simulated curves describe the data, as can be seen in Fig. 9, with modest accuracy. Although at intermediate binding ratios the DNA region between two bound HOE does not appear to be described by a clamped ends model, however we cannot reject the mechanism at higher binding ratios. In fact when fitting the simulated data with the intermediate zone formula decay of Eq. (5), a reasonable fit is obtained for a DNA length longer than 500 base pairs or shorter than 20 (Fig. 9). In particular, when the FPA of a 10 b.p. clamped ends DNA simulated with $\alpha = 5 \times 10^{-12}$ erg is fitted with the intermediate zone formula, an $\alpha^*$ value of $10^{-7}$ erg is found, very close to the experimental value obtained at the highest HOE concentration investigated.

From the discussion of the above assumptions, one can suggest a description of the large increase of the DNA effective torsional constant $\alpha^*$ in the presence of HOE. At the early stages of binding, $[H]/[BP] \leqslant 0.5$, there is a modest increase in $\alpha^*$ similar to that found with chloroquine. The intercalator, however, is not expected to limit the internal motions of DNA in the same way as HOE does due to the different binding mode (HOE wraps in the minor groove) and to the different size of the two probes (HOE occupies 4–5 base pairs). So, in order to alter the torsional dynamics to the extent that chloroquine does, a lower concentration of HOE is required. When $[H]/[BP]$ exceeds 0.5, there occurs a sudden release of EB together with the dramatic increase in $\alpha^*$. From the data of Lootiens et al. [35] and from reported Scatchard plots [36], also confirmed by the authors, it seems that this value of the binding ratio represents the saturation of the specific minor groove binding sites. Above this value it is expected that HOE could bind to DNA by stacking to already bound HOE molecules and by bridging HOE molecules that are separated by a few base pairs [35] (Fig. 10). According to this view, EB binding to DNA becomes more unfavourable at high HOE binding ratios since it requires untwisting of a much more rigid DNA helix.

## 7. Conclusions

Frequency domain FPA, previously applied to different biological systems, proves to be a suitable technique also for applications to DNA dynamics. In particular, as can be seen from the frequency domain simulations shown in Section 3, of the two relevant quantities of FPA, phase differences appear to be more sensitive than modulations to changes of the parameters regulating the fluorescence anisotropy decay.

The relevant parameter of FPA appears to be the characteristic time $\xi$, which is proportional to the product of the elastic constant $\alpha$ and of the rotational friction coefficient $\gamma$. Whilst the rotational friction coefficient is affected by properties such as temperature [39] and viscosity of the solution, $\alpha$, instead, is sensitive to DNA structure and dynamics perturbations. When examining the FPA data of the ethidium–DNA complex in the presence of probes at binding saturation, either chloroquine or hoechst 33258, one finds changes in the parameter $\xi$ that are attributed to $\alpha$.

As shown by results and simulations fitted with the intermediate expression that describes DNA torsions it appears convenient to introduce an effective elastic constant $\alpha^*$ that summarises different effects accompanying the torsional dynamics.

It has been shown that $\alpha^*$ remains constant and close to $\alpha$ until several chloroquines intercalated are bound in a typical DNA segment spanning a torsional wavelength and the effect, although not large, is greater in circularly closed DNAs.

A very different situation has been found when adding hoechst 33258 to the DNA–EB complex as can be argued by the large increase, about $10^5$ times, found for the effective elastic constant $\alpha^*$ at the highest HOE concentration. As it has been discussed, if the change in the torsional dynamics were fully attributed to the elastic constant only through an increase in the elastic modulus, then HOE covered DNA would become as hard as steel! Probably, a co-operation of a few factors is required for the dramatic increase of $\alpha^*$: a modification of DNA radius due to a change of mass, HOE stacking on A–T sites on DNA producing mass dishomogeneity along the chain which lead to variation in the dynamical laws regulating the anisotropy decay, and ultimately, an actual increase in the intrinsic rigidity of DNA. Summarising, bound HOE appears to be very efficient in hindering the torsional motions and this is likely due to be the result of its wrapping in the DNA minor groove where it covers 4–5 base pairs.

These results promises to be valuable in understanding effects on DNA dynamics of protein binding since

it is known that proteins often bind to DNA grooves and, for instance, the transcription factor 'TF1', is known to make DNA 'stiffer' upon binding to it [40].

In conclusion, the present studies suggest that FPA can be a suitable technique for following changes in the torsional dynamics of DNA under various conditions including those when proteins bind to the double helix.

## Acknowledgements

Thanks are due to G. Badaracco for providing the plasmids used in this work and for discussions and to J. Langowski and U. Kapp for DNA purification. We like to acknowledge Nora Lecis for her help during the measurements, together with Marco Gardella for technical support and all the colleagues of the Biospectroscopy laboratory for useful suggestions. Refereeing of the paper, that has helped clarifying DNA torsional dynamics, is gratefully acknowledged.

## References

[1] J.M. Schurr and K.S. Schmitz, Ann. Rev. Phys. Chem. 37 (1986) 271.
[2] J. Langowski, W. Kremer and U. Kapp, Methods Enzym. 211 (1992) 430.
[3] J.G. Elias and D. Eden, Macromolecules 14 (1981) 410.
[4] D. Porschke, E.R. Schmidt, T. Hankeln, G. Nolte and J. Antosiewicz, Biophys. Chem. 47 (1993) 179.
[5] L. Song and J.M. Schurr, Biopolymers 30 (1990) 229.
[6] G. Maret and G. Weill, Biopolymers 22 (1983) 2727.
[7] J. Langowski, B.S. Fujimoto, D.E. Wemmer, A.S. Benight, G. Drobny, J.H. Shibata and J.M. Schurr, Biopolymers 24 (1985) 1023.
[8] M. Hogan, J. Wang, R.H. Austin C.L. Monitto, and S. Hershkowitz, Proc. Natl. Acad. Sci. U.S.A. 79 (1982) 3518.
[9] S.A. Allison, R. Austin and M. Hogan, J. Chem. Phys. 90 (1989) 3843.
[10] P.E. Rouse, J. Chem. Phys. 21 (1953) 1272.
[11] B.H. Zimm, J. Chem. Phys. 24 (1956) 269.
[12] S.A. Allison and J.M. Schurr, Chem. Phys. 41 (1979) 35.
[13] M.D. Barkley and B.H. Zimm, J. Chem. Phys. 70 (1979) 2991.
[14] J.M. Schurr, Chem. Phys. 84 (1984) 71.
[15] M. Collini, G. Chirico and G. Baldini, Biopolymers 32 (1992) 1447.
[16] P. Wu, L. Song, B. Clendenning, B.H. Fujimoto, A.S. Benight and J.M. Schurr, Biochem. 27 (1988) 8128.
[17] P. Wu and J.M. Schurr, Biopolymers 28 (1989) 1695.
[18] M. Hogan, N. Dattagupta and D.M. Crothers, Proc. Natl. Acad. Sci. USA 75 (1979) 195.
[19] J.H. Shibata, B.S. Fujimoto and J.M. Schurr, Biopolymers 24 (1985) 1909.
[20] L. Song, S.A. Allison and J.M. Schurr, Biopolymers 29 (1990) 1773.
[21] B.S. Fujimoto and J.M. Schurr, Nature 344 (1990) 175.
[22] P. Wu, B.S. Fujimoto and J.M. Schurr, Biopolymers 26 (1987) 1463.
[23] G. Weber, J. Chem. Phys. 66 (1977) 4081.
[24] J.R. Lakowicz, Principles of fluorescence spectroscopy (Plenum Press, New York, 1983)
[25] H. Szmacinski, R. Jayaweera, H. Cerek and J.R. Lakowicz, Biophys. Chem. 27 (1987) 233
[26] R.D. Ludescher, L. Peting, S. Hudson and B. Hudson, Biophys. Chem. 28 (1987) 59.
[27] B.P. Maliwal and J.R. Lakowicz, Biochim. Biophys. Acta 873 (1986) 161.
[28] G. Chirico, S. Beretta and G. Baldini, Biophys. Chem. 45 (1992) 101.
[29] J.R. Lakowicz and B.P. Maliwal, Biophys. Chem. 21 (1985) 61.
[30] R.L. Jones, A.C. Lanier, R.A. Keel and W.D. Wilson, Nucleic Acid Res. 8 (1980) 1613.
[31] B. Weisblum and E. Haenssler, Chromosoma 46 (1974) 255.
[32] R.F. Steiner and H. Stenberg, Archives Biochem. Biophys. 197 (1979) 580.
[33] S.A. Latt and J.C. Wohlleb, Chromosoma 52 (1975) 297.
[34] S.A. Latt, Can. J. Genet. Cytol. 19 (1977) 603.
[35] F.G. Lootiens, P. Regenfuss, A. Zechel, L. Dumortier and R.M. Clegg, Biochem. 29 (1990) 9029.
[36] M.V. Mikhailov, A.S. Zasedatelev, A.S. Krylov and G.V. Gurskii, J. Mol. Biol. 15 (1981) 54.
[37] P.E. Pjura, K. Grzeskowiak and R.E. Dickerson, J. Mol. Biol. 197 (1987) 257.
[38] D.E. Comings, Chromosoma 52 (1975) 229.
[39] J.C. Thomas and J.M. Schurr, Biochem. 22 (1983) 6194.
[40] T. Härd and D.R. Kearns, Biochem. 29 (1990) 959.